

UDC: 534:699.844:331.45

OECD: OECD: 01.03. AA

## Evaluation of the sound insulation properties of a lightweight panel with an internal diamond-shaped structure based on computer modeling of the process of passage and absorption of sound energy in it

Asminin V.F.<sup>1</sup>, Druzhinina E.V.<sup>2</sup>, Sazonova S.A.<sup>3\*</sup>

<sup>1</sup> DSc., Professor, Department of 'Life Safety and Legal Relations'

<sup>2</sup> Lecturer, Department of 'Life Safety and Legal Relations'

<sup>3</sup> PhD, Associate Professor, Department of 'Technosphere and Fire Safety'

<sup>1,2</sup> Voronezh State Forestry University named after G.F. Morozov, Voronezh, Russia

<sup>3</sup> Voronezh State Technical University, Voronezh, Russia

### Abstract

Acoustic screens used in industrial enterprises for noise reduction and creation of comfortable working conditions are considered. It is proposed to use a new design of a portable lightweight soundproofing panel with a corrugated diamond-shaped structure. The results of mathematical modeling of the process of sound transmission and distribution in a portable lightweight soundproof panel are presented. Simulation of sound distribution in the studied medium was performed by applying a mesh model with concentrated parameters. The mathematical model is a system of differential equations, the solution of which makes it possible to determine the mechanical behavior of the system based on the given parameters. The Runge-Kutta second order method was used for the numerical implementation of the mathematical model. An analytical formula for the nodes in the design scheme depending on the parameters of the sound-isolating panel under study is obtained. The developed model, due to its versatility, allows modeling the sound distribution with a wide variety of characteristics. Three types of sounds for conducting basic computer experiments were selected: sinusoidal, single pulse of rectangular shape, single pulse of Gaussian shape. The calculation of sound absorption characteristics is performed. An algorithm for the passage of sound through a sound-isolating panel has been developed. Initial and boundary conditions, model assumptions are given. The software implementation of the model has been performed. The results of computer modeling, proving the effective sound absorption of the proposed portable lightweight soundproof panel are presented and analyzed.

**Keywords:** acoustic screens, sound insulation, portable lightweight soundproof panel with diamond-shaped structure, mathematical modeling, computer experiment.

### Оценка звукоизолирующих свойств облегченной панели с внутренней ромбовидной структурой на основе компьютерного моделирования процесса прохождения и поглощения в ней звуковой энергии

Асминин В.Ф.<sup>1</sup>, Дружинина Е.В.<sup>2</sup>, Сазонова С.А.<sup>3\*</sup>

<sup>1</sup> Д.т.н., профессор кафедры «Безопасность жизнедеятельности и правовых отношений»

<sup>2</sup> Преподаватель кафедры «Безопасность жизнедеятельности и правовых отношений»

<sup>3</sup> К.т.н., доцент кафедры «Техносферная и пожарная безопасность»

<sup>1,2</sup> ФГБОУ ВО «Воронежский государственный лесотехнический университет им. Г.Ф. Морозова», г. Воронеж, РФ

<sup>3</sup> ЗФГБОУ ВО «Воронежский государственный технический университет», г. Воронеж, РФ

### **Аннотация**

Исследуются акустические свойства звукоизоляционных экранов, используемых на промышленных предприятиях для снижения уровня шума и создания требуемых условий труда. Предлагается использовать новый тип портативной легкой звукоизоляционной плиты с гофрированной ромбовидной структурой. Рассмотрены результаты моделирования процесса передачи и распространения звука в портативных легких звукоизоляционных панелях. Сетчатая расчетная модель с дискретными параметрами использовалась для моделирования распространения звука в исследуемой среде. Математическая модель состоит из системы дифференциальных уравнений, решение которой позволяет определять механическое поведение системы на основе заданных параметров. Метод Рунге-Кутты второго порядка использовался для численной реализации предложенной математической модели. В соответствии с параметрами исследуемой звукоизоляционной плиты была получена аналитическая формула для узлов в расчетной схеме. Предложенная модель, благодаря своей универсальности, позволяет моделировать распространение звука с самыми разнообразными характеристиками. При проведении базовых компьютерных экспериментов были выбраны три типа звуков: синусоидальные, одиночный импульс прямоугольной формы и одиночный импульс гауссовой формы. В результате проведенных исследований были определены характеристики звукопоглощения. Был разработан алгоритм прохождения звука через звукоизоляционные панели. В статье приведены начальные и граничные условия и допущения для модели. После программной реализации модели были проанализированы результаты компьютерного моделирования, позволяющие сделать вывод о эффективности звукопоглощающей способности предлагаемой портативной легкой звукоизоляционной плиты.

**Ключевые слова:** акустические экраны, звукоизоляция, переносная облегчённая звукоизолирующая панель с ромбовидной структурой, математическое моделирование, компьютерный эксперимент.

### **Introduction**

Acoustic screens (hereinafter referred to as AS) have a noise-canceling effect, as they effectively protect workers from the direct effects of noise. They are installed between the noise sources and the workplace in order to create a shadow area where sound waves penetrate only partially.

The sound-proofing properties of the screen material, which depend on its density, are of great importance in the effectiveness of its application. As it is known, the greater the density and thickness of the material, the higher the sound insulation of the structure.

Stationary acoustic screens in production workshops have not found wide application, for the same reason as wall sound-proofing walls.

Portable acoustic screens for permanent and temporary workplaces are rarely used due to:

- their large weight and dimensions;
- inconveniences of movement and transportation;
- difficulties arising in their storage and storage when there is no need to use them (for example, at temporary workplaces).

Based on experimental studies, it was found that the design of a portable lightweight soundproof panel (PLS panel) with a corrugated diamond-shaped structure is the most effective one.

PLS panels with a corrugated diamond-shaped structure are proposed to be made from

polymer film materials or from leafed pulp and paper materials, fabrics (Figures 1 and 2) [1].

Figure 1 shows a general view of the PLS panel in an axonometric projection. Figure 2 schematically shows the process of folding the panel during disassembly for storage or transfer to another room. The PLS panel contains a diamond-shaped partition 1 enclosed between two parallel flat partitions 2 and 3, which have bending lines 4.

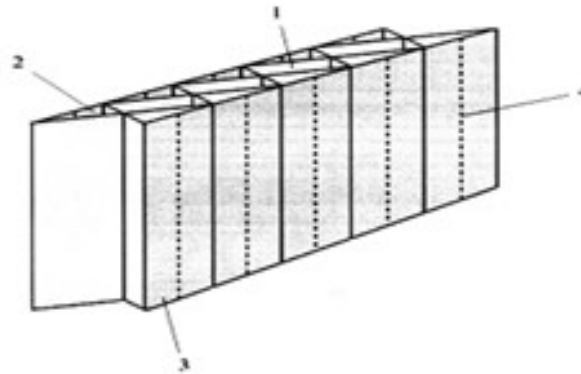


Fig. 1. General view of the PLS panel

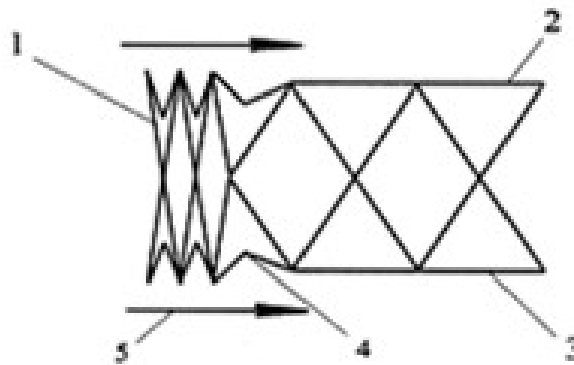


Fig. 2. Cross section of the PLS panel structure during the disassembly process

### 1. Simulation of the process of sound transmission and distribution in the PLS panel

To study the process of sound transmission and distribution in the PLS panel, as well as to confirm the acoustic efficiency of the developed structure, its computer simulation considering certain assumptions and limitations is proposed. To simulate the propagation of sound in the PLS panel and its scattering, the studied media were presented in the form of a grid model with concentrated parameters (Figure 3).

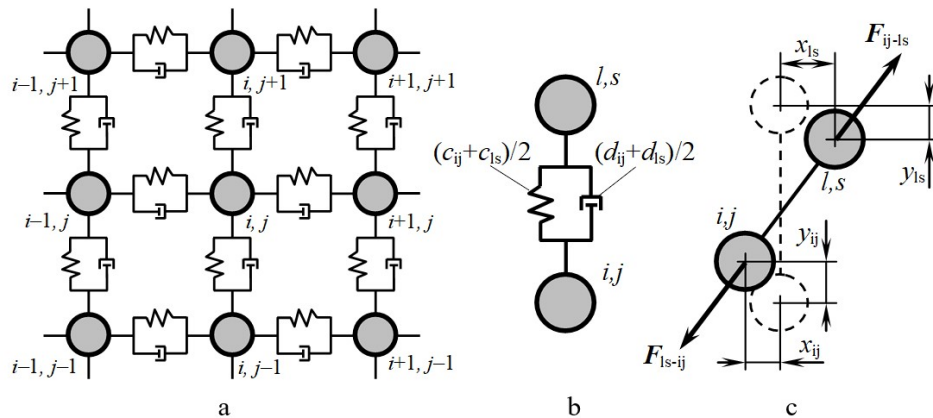


Fig. 3. Rectangular grid used in the model: a – indexing of grid nodes; b – separate viscoelastic interaction; c – the appearance of elastic forces when the grid nodes are displaced from equilibrium positions

The following parameters are used for grid nodes:

- parameter of the medium type  $k_{ij}$  (for the panel material  $k_{ij} = 1$ , for the air medium  $k_{ij} = 0$ );
- the mass parameter  $m_{ij}$ , wherein  $m = \rho d_0^3$ ,  $\rho$  is the volume density of the medium;
- the Cartesian components of the displacement  $x_{ij}$ ,  $y_{ij}$  represent the displacement of the node from its equilibrium position in the horizontal and vertical planes;
- the Cartesian components of the velocity  $v_{xij}$ ,  $v_{yij}$  describe the displacement velocity of the node in the horizontal and vertical planes;
- the coefficient of rigidity of the interaction  $c_{ij}$  determines the degree of rigidity of the connection between the nodes of the grid;
- the viscosity coefficient of the interaction  $d_{ij}$  reflects the degree of damping of the connection between the nodes.

Below, the grid dimensions are denoted by  $n \times m$  ( $i = 1 \dots n$ ,  $j = 1 \dots m$ ). Figure 4 shows the model representation of the media through which the sound passes.

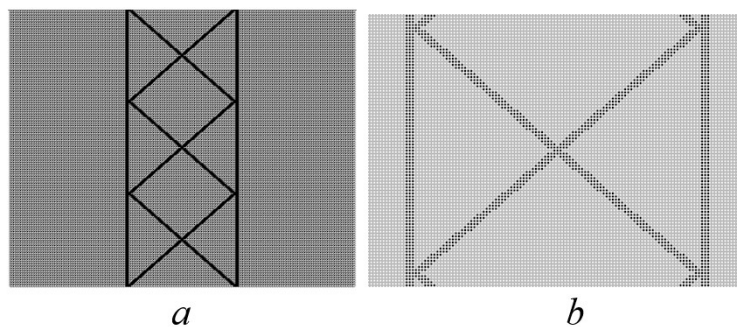


Fig. 4. Model representation of the medium for sound distribution in the form of a straight-angle grid with nodes of two types (air and material of the panel are, respectively, white and black circles): a – fully simulated system (three panel element cells); b – enlarged middle panel cell

Equations (1) constitute a system of differential equations, the solution of which makes it possible to determine the mechanical behavior of the system based on the given parameters (masses, stiffness, friction coefficients, etc.).

$$\left\{ \begin{aligned}
 m_{ij} \frac{d^2 x_{ij}}{dt^2} &= \frac{c_{ij} + c_{i+1j}}{2} \left( d_0 - \sqrt{(x_{i+1j} - x_{ij})^2 + (y_{i+1j} - y_{ij})^2} \right) \frac{x_{i+1j} - x_{ij}}{\sqrt{(x_{i+1j} - x_{ij})^2 + (y_{i+1j} - y_{ij})^2}} + \\
 &+ \frac{c_{ij} + c_{i-1j}}{2} \left( d_0 - \sqrt{(x_{i-1j} - x_{ij})^2 + (y_{i-1j} - y_{ij})^2} \right) \frac{x_{i-1j} - x_{ij}}{\sqrt{(x_{i-1j} - x_{ij})^2 + (y_{i-1j} - y_{ij})^2}} + \\
 &+ \frac{c_{ij} + c_{ij+1}}{2} \left( d_0 - \sqrt{(x_{ij+1} - x_{ij})^2 + (y_{ij+1} - y_{ij})^2} \right) \frac{x_{ij+1} - x_{ij}}{\sqrt{(x_{ij+1} - x_{ij})^2 + (y_{ij+1} - y_{ij})^2}} + \\
 &+ \frac{c_{ij} + c_{ij-1}}{2} \left( d_0 - \sqrt{(x_{ij-1} - x_{ij})^2 + (y_{ij-1} - y_{ij})^2} \right) \frac{x_{ij-1} - x_{ij}}{\sqrt{(x_{ij-1} - x_{ij})^2 + (y_{ij-1} - y_{ij})^2}} + \\
 &+ \frac{d_{ij} + d_{i+1j}}{2} \left( \frac{dx_{i+1j}}{dt} - \frac{dx_{ij}}{dt} \right) + \frac{d_{ij} + d_{i-1j}}{2} \left( \frac{dx_{i-1j}}{dt} - \frac{dx_{ij}}{dt} \right) + \\
 &+ \frac{d_{ij} + d_{ij+1}}{2} \left( \frac{dx_{ij+1}}{dt} - \frac{dx_{ij}}{dt} \right) + \frac{d_{ij} + d_{ij-1}}{2} \left( \frac{dx_{ij-1}}{dt} - \frac{dx_{ij}}{dt} \right); \\
 m_{ij} \frac{d^2 y_{ij}}{dt^2} &= \frac{c_{ij} + c_{i+1j}}{2} \left( d_0 - \sqrt{(x_{i+1j} - x_{ij})^2 + (y_{i+1j} - y_{ij})^2} \right) \frac{y_{i+1j} - y_{ij}}{\sqrt{(x_{i+1j} - x_{ij})^2 + (y_{i+1j} - y_{ij})^2}} + \\
 &+ \frac{c_{ij} + c_{i-1j}}{2} \left( d_0 - \sqrt{(x_{i-1j} - x_{ij})^2 + (y_{i-1j} - y_{ij})^2} \right) \frac{y_{i-1j} - y_{ij}}{\sqrt{(x_{i-1j} - x_{ij})^2 + (y_{i-1j} - y_{ij})^2}} + \\
 &+ \frac{c_{ij} + c_{ij+1}}{2} \left( d_0 - \sqrt{(x_{ij+1} - x_{ij})^2 + (y_{ij+1} - y_{ij})^2} \right) \frac{y_{ij+1} - y_{ij}}{\sqrt{(x_{ij+1} - x_{ij})^2 + (y_{ij+1} - y_{ij})^2}} + \\
 &+ \frac{c_{ij} + c_{ij-1}}{2} \left( d_0 - \sqrt{(x_{ij-1} - x_{ij})^2 + (y_{ij-1} - y_{ij})^2} \right) \frac{y_{ij-1} - y_{ij}}{\sqrt{(x_{ij-1} - x_{ij})^2 + (y_{ij-1} - y_{ij})^2}} + \\
 &+ \frac{d_{ij} + d_{i+1j}}{2} \left( \frac{dy_{i+1j}}{dt} - \frac{dy_{ij}}{dt} \right) + \\
 &+ \frac{d_{ij} + d_{i-1j}}{2} \left( \frac{dy_{i-1j}}{dt} - \frac{dy_{ij}}{dt} \right) + \frac{d_{ij} + d_{ij+1}}{2} \left( \frac{dy_{ij+1}}{dt} - \frac{dy_{ij}}{dt} \right) + \frac{d_{ij} + d_{ij-1}}{2} \left( \frac{dy_{ij-1}}{dt} - \frac{dy_{ij}}{dt} \right).
 \end{aligned} \right. \quad (1)$$

Second order differential equations (1) are solved by the second order Runge-Kutta method [2]:

$$\begin{aligned}
 x_{ij}^{\tau+1} &= x_{ij}^{\tau} + v_{xij}^{\tau} \cdot \Delta t + a_{xij}^{\tau} \cdot (\Delta t)^2 / 2; \\
 v_{xij}^{\tau+1} &= v_{xij}^{\tau} + a_{xij}^{\tau} \cdot \Delta t; \\
 y_{ij}^{\tau+1} &= y_{ij}^{\tau} + v_{yij}^{\tau} \cdot \Delta t + a_{yij}^{\tau} \cdot (\Delta t)^2 / 2; \quad v_{yij}^{\tau+1} = v_{yij}^{\tau} + a_{yij}^{\tau} \cdot \Delta t,
 \end{aligned} \quad (2)$$

wherein  $x_{ij}, v_{ij}, a_{ij}$  are the coordinate, speed, acceleration of the node, respectively;  $\Delta t$  is the time integration step;  $ij$  are the node indices,  $\tau$  and  $\tau + 1$  are the indices of the current and next time step.

## 2. Model representation of the soundproof panel

We set the node type  $k_{ij} = 1$  (panel material) to those nodes that fall into the geometric area corresponding to the panel. For the other nodes, the node type  $k_{ij} = 0$  (the air) is set.

We obtain an analytical formula for  $k_{ij}$  depending on the parameters of the soundproof panel (panel thickness  $a$ ; cell size  $b$ ; thickness of the front/rear wall  $d_C$ , the thickness of the partition  $d_{II}$ ) (Figure 5).

$$k_{ij} = \begin{cases} 1, & \left[ \begin{array}{l} \left\{ \begin{array}{l} \frac{b}{a} \left| i - \frac{n}{2} \right| d_0 - \frac{d_{II}}{2} \frac{\sqrt{a^2+b^2}}{b} < (j - \frac{m}{2}) d_0 + bN_{\mathcal{R}} < \frac{b}{a} \left| i - \frac{n}{2} \right| d_0 + \frac{d_{II}}{2} \frac{\sqrt{a^2+b^2}}{b}; \\ \left| i - \frac{n}{2} \right| d_0 < a + \frac{d_C}{2}; \end{array} \right. \\ \left\{ \begin{array}{l} -\frac{b}{a} \left| i - \frac{n}{2} \right| d_0 - \frac{d_{II}}{2} \frac{\sqrt{a^2+b^2}}{b} < -(j - \frac{m}{2}) d_0 + bN_{\mathcal{R}} < -\frac{b}{a} \left| i - \frac{n}{2} \right| d_0 + \frac{d_{II}}{2} \frac{\sqrt{a^2+b^2}}{b}; \\ \left| i - \frac{n}{2} \right| d_0 < a + \frac{d_C}{2}; \end{array} \right. \\ \left\{ \begin{array}{l} \frac{b}{2s} \left| i - \frac{n}{2} \right| d_0 + \frac{b}{2} - \frac{ab}{s} - \frac{d_C}{2} \frac{\sqrt{4s^2+b^2}}{b} < (j - \frac{m}{2}) d_0 + bN_{\mathcal{R}} < \frac{b}{2s} \left| i - \frac{n}{2} \right| d_0 + \frac{b}{2} - \frac{ab}{s} + \frac{d_C}{2} \frac{\sqrt{4s^2+b^2}}{b}; \\ \frac{a}{2} - s - \frac{d_C}{2} < \left| i - \frac{n}{2} \right| d_0 < \frac{a}{2}; \\ (j - \frac{m}{2}) d_0 + bN_{\mathcal{R}} < \frac{b}{2}; \end{array} \right. \\ \left\{ \begin{array}{l} -\frac{b}{2s} \left| i - \frac{n}{2} \right| d_0 - \frac{b}{2} + \frac{ab}{s} - \frac{d_C}{2} \frac{\sqrt{4s^2+b^2}}{b} < -(j - \frac{m}{2}) d_0 + bN_{\mathcal{R}} < -\frac{b}{2s} \left| i - \frac{n}{2} \right| d_0 - \frac{b}{2} + \frac{ab}{s} + \frac{d_C}{2} \frac{\sqrt{4s^2+b^2}}{b}; \\ \frac{a}{2} - s - \frac{d_C}{2} < \left| i - \frac{n}{2} \right| d_0 < \frac{a}{2}; \\ -(j - \frac{m}{2}) d_0 + bN_{\mathcal{R}} > -\frac{b}{2}; \end{array} \right. \end{array} \right. \\ 0, \text{ otherwise} \end{cases} \quad (3)$$

wherein  $N_{\mathcal{R}}$  is the panel cell number (in most calculations,  $N_{\mathcal{R}}$  took the values  $-1, 0, 1$ ).

The main cell of the soundproof panel is located in the center of the model space (Figure 5): the point  $O$  has the coordinates  $(n/2 \cdot d_0, m/2 \cdot d_0)$ .

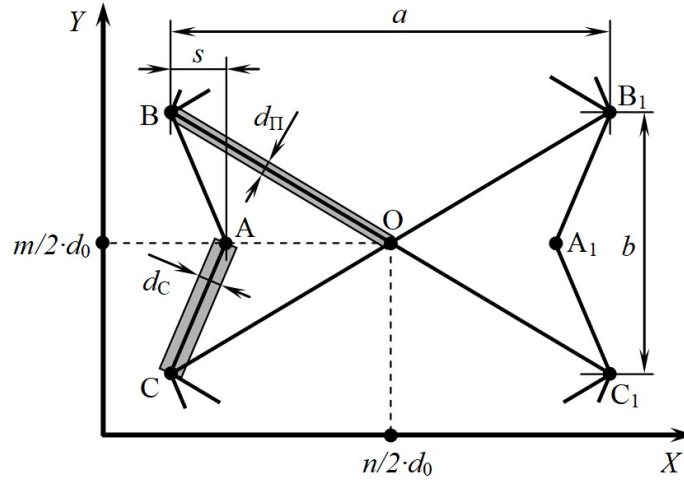


Fig. 5. Model representation of the soundproof panel

### 3. Model representation of the sound source and receiver

The developed model can be used to study the propagation of sound in various media, such as air, water, solids and others. It also takes into account various physical properties of the medium, such as the density and speed of sound. Due to this, the model can be used to analyze and predict sound phenomena such as noises, echoes and resonance. It can also be used to optimize the acoustic design of rooms and the development of sound-absorbing materials [3,4].

The high versatility of the developed model makes it an effective tool for exploring and improving the sound environment.

For basic computer experiments, the model reproduces the incident of a plane sound wave on a sound-absorbing panel, for which the coordinates of nodes located in the leftmost row (having indices  $i = 1, j - \text{arbitrary}$ ) are simultaneously changed. The sound source is given by a mathematical expression for the function  $x_{1j}(t)$ .

Three types of sounds were selected for carrying out the basic computer experiments:

a) sinusoidal, given by the formula

$$x_{1j}(t) = A_3 \sin \left( \frac{2\pi}{f_3} t \right), \quad (4)$$

wherein  $A_3$  and  $f_3$  are the amplitude and frequency of sound;

b) a single pulse of rectangular shape:

$$x_{1j}(t) = A_{\text{H}} \begin{cases} 0, & t < t_{\text{H}}; \\ 1, & t_{\text{H}} \leq t < t_{\text{H}} + t_{\text{H}}; \\ 0, & t \geq t_{\text{H}} + t_{\text{H}}, \end{cases} \quad (5)$$

wherein  $A_{\text{H}}$  is the pulse amplitude;  $t_{\text{H}}$  is the moment of time at which the pulse is emitted;  $t_{\text{H}}$  is the pulse duration.

c) a single pulse of Gaussian shape:

$$x_{1j}(t) = A_{\text{H}} e^{-\frac{(t-t_0)^2}{\tau_{\text{H}}}}, \quad (6)$$

wherein  $\tau_{\text{H}}$  is the parameter describing the pulse duration (the pulse duration is approximately equal to  $6\tau_{\text{H}}$ );  $t_0$  is the moment when the pulse amplitude reaches its maximum.

The current sound level  $x_{\text{H}}(t) \times N(t)$  perceived by the model 'receiver' is determined by averaging the horizontal displacements  $x_{nj}(t)$  of nodes with the index 'nj' (index  $i = n$  means the maximum index in the direction  $i$ ):

$$x_{\text{H}}(t) = \frac{1}{m} \sum_{j=1}^n |x_{nj}(t)|, \quad (7)$$

wherein  $m$  is the maximum index of nodes in the vertical direction ( $j = 1 \dots m$ ).

The amplitude of the received sound  $A_{\text{H}}$  is defined as the maximum value of the function  $x_{\text{H}}(t)$ :

$$A_{\text{H}} = \max_t \left( \frac{1}{m} \sum_{j=1}^n |x_{nj}(t)| \right) \quad (8)$$

From comparing the amplitude of the sound of the transmitter  $A_3$  and the sound of the receiver  $A_{\text{H}}$ , we can conclude about the effectiveness of sound absorption when passing through the medium. Quantitatively, this efficiency is expressed in terms of the logarithmic attenuation increment  $\theta = \lg(A_3/A_{\text{H}})$  and is expressed in decibels (dB).

Each step of the calculation is based on the previous values and uses numerical methods to approximate the desired parameters. That is, the model uses numerical methods and algorithms to calculate output characteristics based on sampling of input data. Analytical models, on the contrary, are based on analytical transformations of mathematical equations, which may be impossible for complex simulated processes. A simplified calculation algorithm is presented in the flowchart (Figure 6).

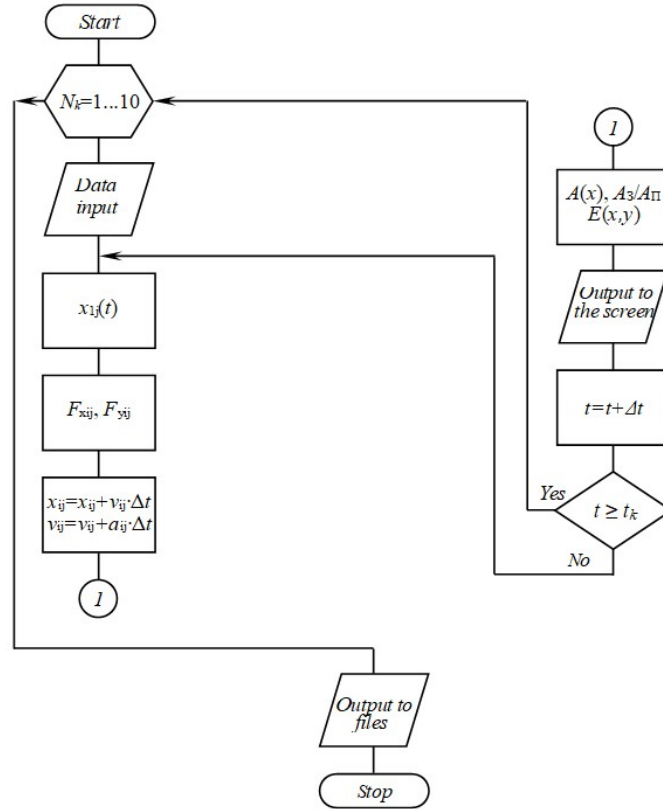


Fig. 6. The algorithm of sound transmission through the soundproof PLS panel

#### 4. Calculation of sound absorption characteristics

Because the developed model reproduces sound distribution at the level of vibration of individual nodes, there are ample opportunities to determine various characteristics of the sound transmission process through the panel. In particular, the following characteristics are used for further analysis:

- the amplitude of the sound after the passage of the panel  $A_{\Pi}$  (or the logarithmic decay of the sound during the passage of the panel  $\theta = \lg(A_3/A_{\Pi})$ );
- the dependence of the sound amplitude along the line perpendicular to the plane of the panel  $A(x)$ .
- the dependence of the displacements of the control elements on time  $x_{ij}(t)$ .
- the scheme of the current displacements of the elements of the medium  $x(i,j,t)$ ;
- the scheme of the current energy distribution in the medium  $E(x,y,t)$ , defined as follows:

$$E(x,y,t) = E(id_0, jd_0, \tau) = E_{\Pi ij}^{\tau} + E_{K ij}^{\tau} = \frac{c_{ij}}{2} \left( (x_{ij}^{\tau})^2 + (y_{ij}^{\tau})^2 \right) + \frac{m_{ij}}{2} \left( (v_{xij}^{\tau})^2 + (v_{yij}^{\tau})^2 \right), \quad (9)$$

wherein  $E_{\Pi ij}$  and  $E_{K ij}$  is the potential and kinetic energy of the element  $ij$ .

#### 5. Initial and boundary conditions, model assumptions

##### 5.1. Initial conditions

At the initial moment of time, the offsets  $x, y$  and node velocities are equal to zero:

$$x_{ij}^0 = 0, y_{ij}^0 = 0, v_{xij}^0 = 0, v_{yij}^0 = 0.$$

### 5.2. Boundary conditions

Nodes on the upper ( $j = m$ ), lower ( $j = 1$ ) and right ( $i = n$ ) boundaries of the model space are fixed:

$$x_{i1} = 0; y_{i1} = 0; x_{im} = 0; y_{im} = 0; x_{nj} = 0; y_{nj} = 0;$$

$$v_{xi1} = 0; v_{yi1} = 0; v_{xim} = 0; v_{yim} = 0; v_{xnj} = 0; v_{ynj} = 0.$$

Nodes on the left boundary ( $i = 1$ ) of the model space move according to a given law (see above) – in accordance with the nature of the sound being supplied.

### 5.3. For the model, we introduce the following assumptions:

- the environment is considered as solid;
- the physical properties of the medium extend to all nodes and the connections between them;
- the interaction between nodes is considered linear viscoelastic, which means that the connections between nodes have both elastic and viscous characteristics;
- the nodes of the model perform mechanical movement near equilibrium positions according to the laws of classical dynamics, that is, the movement of the nodes is determined by Newton's laws;
- the modeling does not take into account the effect of gravity on the environment, which means that the gravitational influence is not taken into account when calculating the model;
- the mechanical properties of the material depend only on five parameters of the elements: mass, diameter, viscosity coefficients, stiffness coefficients and interaction constraints. This means that the properties of the material used in the model are determined only by these five parameters.

## 6. Software implementation of the model

The developed mathematical model is numerically implemented using the computer program 'A program for modeling the passage of sound through a lightweight soundproof panel with a corrugated diamond-shaped structure', which is developed in the Object Pascal language in the integrated programming environment Borland Delphi 7.0 (Figure 7).

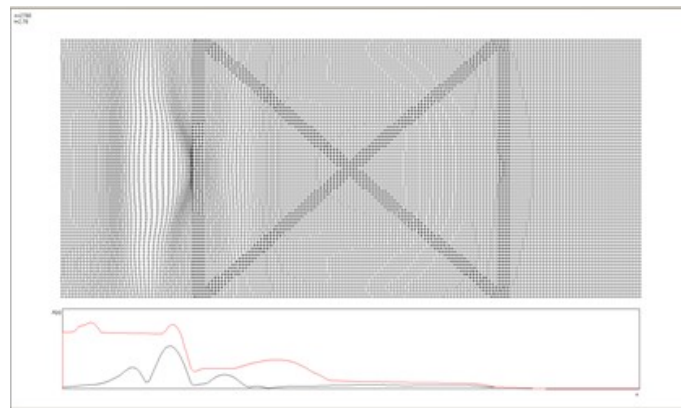


Fig. 7. The form of the output of the computer experiment results in the developed program

The program is designed to study and simulate the passage of sound through panels with a corrugated diamond-shaped structure. It can be useful when designing sound insulation systems, such as insulation panels for rooms or sound-absorbing materials.

After the computer experiment was completed, the program recorded the main characteristics of the process (the distribution of the sound amplitude in the direction perpendicular to the plane of the panel, the time dependence of the amplitude of the vibrations of air particles before and after passing the panel) in files on the hard disk of the computer.

## 7. Features of the computer experiment

The numerical experiment consisted in modeling the distribution of a given initial air vibration through a soundproof panel and determining the nature of the air vibrations behind the panel.

During the computer experiment, the disturbance of the air environment, initially created on the left boundary of the model space, moved at a certain speed in the direction of the panel, then the disturbance was transmitted to the panel itself, causing complex deformations of the structure [5-8].

Spreading inside the panel, the disturbance at a certain point in time came out from the right side of the panel, causing fluctuations in the air environment. At a given distance from the panel, on the right side, there were a number of elements, the average displacement of which determined the amplitude of the transmitted sound AP.

## 8. Investigation using the acoustic efficiency model of the PLS panel

### 8.1. Stages of the process of overcoming the PLS panel by the sound

To analyze the process of overcoming the PLS panel by sound using the developed model, a sequence of energy distribution schemes  $E(x, y, t)$  and displacements  $x_{ij}(x, y, t)$  at several key points in time was obtained (Figures 8-11).

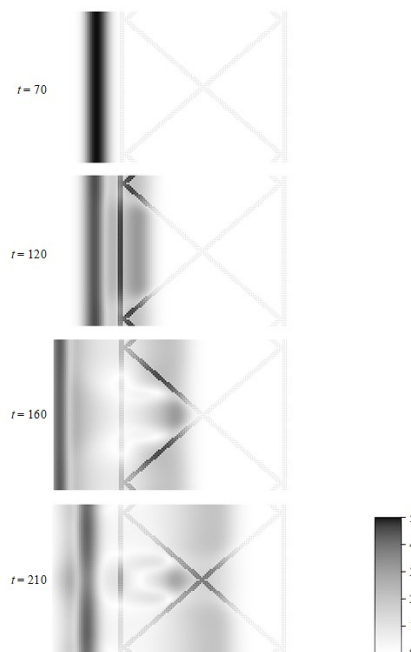


Fig. 8. Scheme of the sound energy distribution as it passes through the PLS panel

For the convenience of visual analysis of the process, the passage of a Gaussian-shaped sound pulse with a characteristic width of about 3 cm was simulated in the model.

The width of the pulse was specially chosen for a comparable smaller panel thickness (45 or 90 mm, depending on the purpose of the computer experiment), in order for the passage of the pulse to be observed more clearly. In addition, for this computer experiment, the density of the panel material was specially significantly reduced and amounted to 1/10 of the density of air. The reason was that for the real density of the panel material, even one thin wall leads to a significant decrease in the amplitude of the sound, which would complicate the visual analysis of the energy distribution scheme s and the displacement of the medium.

Such steps to improve the presentation qualities of the model were made only for the first computer experiments. For the main series of computer experiments, the density of the panel material corresponded to the real density of polyethylene (or cardboard), and the width of the sound pulses corresponded to the frequency of 1000 Hz (the most characteristic frequency of sound).

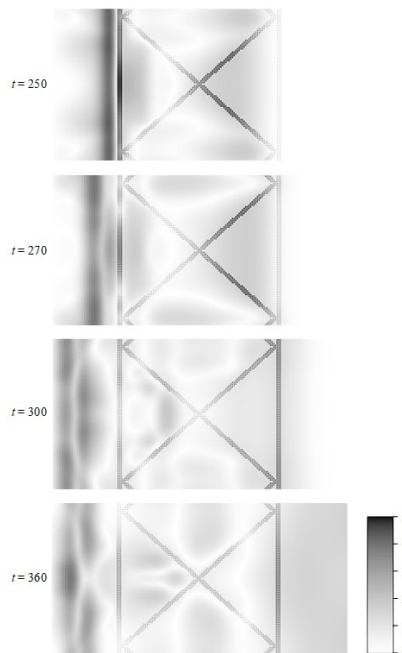


Fig. 9. Scheme of sound energy distribution as it passes through the PLS panel

It should also be noted that in Figures 10, 11 the displacements of the elements of the medium are depicted magnified by 1000 times for the convenience of visual analysis. In reality, the amplitude of the initial sound pulse was 100 dB.

Now consider the stages of the process of overcoming the PLS panel by the sound. Initially, the sound is a Gaussian-shaped air disturbance moving at the speed of sound in the air in the direction of the panel (Figures 8, 10,  $t = 70$  microseconds).

At the moment of contact of the sound pulse with the panel's outer wall, peculiar membranes are formed on the wall – free sections of the wall resting on the junction of the wall with the internal partitions (Figures 8, 10,  $t = 120$  microseconds). The membranes partially transmit the disturbance of the medium inside the panel (into the triangular air chamber), partially reflect the disturbance from the panel. The junctions of the wall and partitions also act as a secondary sound source and transmit perturbation both along the partitions and into the air chamber of the rhombic section.

Further, the sound inside the panel passes through three mechanisms (Figures 8, 10,  $t = 160$  microseconds).

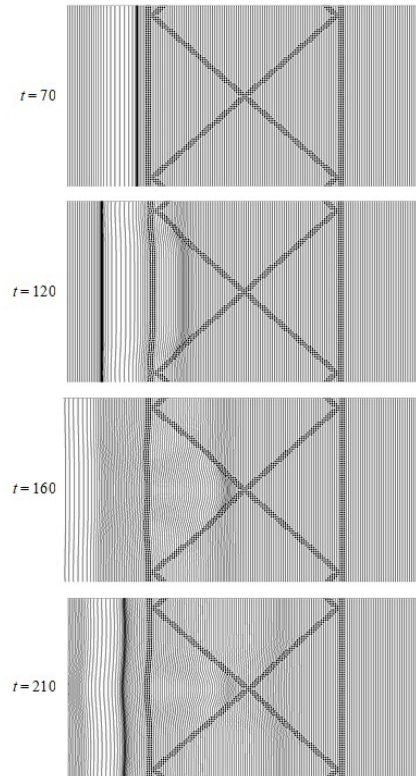


Fig. 10. Offset of the PLS panel elements during the sound passage

When the disturbance reaches the center of the panel, the following effects occur (Figures 8, 10,  $t = 210$  microseconds):

a) in an air chamber of triangular cross-section, a focused disturbance acts on a strong central node of the intersection of internal overheating. As a result, the sound energy spread in the chamber air is significantly dissipated by internal friction in the partition material. Part of the sound disturbance is transmitted to the central node, and it further acts as a point source of sound in the second triangular air chamber;

b) the disturbance propagating along the partitions continues to spread further after overcoming the central node, continuing to lose energy to internal friction in the material of the superglue;

c) in the rhombic chamber, the air disturbance has a width (judging by the dimming on the energy distribution scheme) about twice as large as the outgoing sound pulse.

By the time the outer wall is reached, the following effects occur (Figures 9, 11,  $t = 250, 270$  microseconds):

a) sound is focused in the rhombic chamber and the disturbance hits the solid junction of the internal partitions with the far outer wall, due to which a significant damping of the disturbance occurs;

b) disturbances moving along the internal partitions reach the junction of the partitions with the far outer wall, and are transmitted to these nodes;

c) in the distant triangular chamber, the sound, propagating mainly from a point source, is additionally blurred in time and the sound pulse has a width approximately three to four times greater than the original pulse. This blurred pulse is transmitted to an extended section of the far outer wall, which acts as a membrane, relying on the nodes of the connection of the outer wall with internal partitions.

After contact with the outer wall, the disturbance of the medium is partially reflected back into the panel, partially exits the panel and continues to propagate in the air in the form of

a flat single wave (Figures 9, 11,  $t = 300, 360$  microseconds). It should be noted that the sound pulse after passing the panel is significantly blurred (judging by the width of the darkening area - at least 4 times).

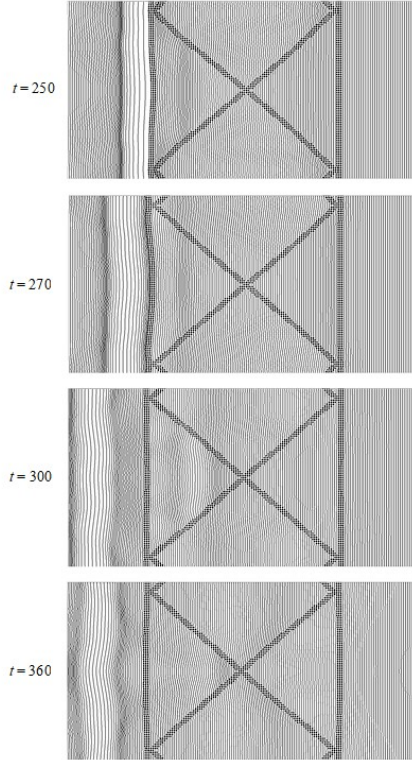


Fig. 11. Offset of the PLS panel elements during the passage of sound

As the sound disturbance passes through the PLC panel, due to the internal structure of the panel, more than 10 effects are observed, each of which leads to a damping of the disturbance energy, or to a blurring of the disturbance in time.

## 8.2. Influence of frequency and amplitude of sound

For practical use, the proposed PLS panel should provide sufficiently high sound absorption in a wide range of frequency and amplitude of sound. In order to determine the effect of the sound frequency  $f_3$  on the sound absorption efficiency, a series of computer experiments on the passage of a sinusoidal sound wave in the following octave frequency bands  $f_3$  was carried out: 125, 250, 500, 1000, 2000, 4000, 8000, 16000 Hz. Figure 12 shows the dependence of the sound pressure level  $L$  after passing the panel from the speaker. For comparison, the experimental dependence  $I(f_3)$  is also depicted.

The dependence  $L(f_3)$  has a maximum in the frequency range of 500-2000 Hz, which indicates the lowest absorption capacity of the panel in this range.

The best absorption is observed in the frequency range of less than 500 Hz and more than 4000 Hz. The model dependence coincides well with the experimental one both qualitatively (the characteristic form of the curve with a wide maxim is reproduced) and quantitatively (on average, the difference is about 7%).

The greatest difference is observed in the low frequency region (in particular 125 Hz) and is associated with the complexity of reproducing sound waves in the model with a large wavelength significantly exceeding the size of the modeling area.

A good coincidence of model and experimental data indicates a high adequacy of the model. In the entire range of frequencies under consideration, the PLS panel absorbs sound quite effectively and has the greatest efficiency in the low and high frequency regions.

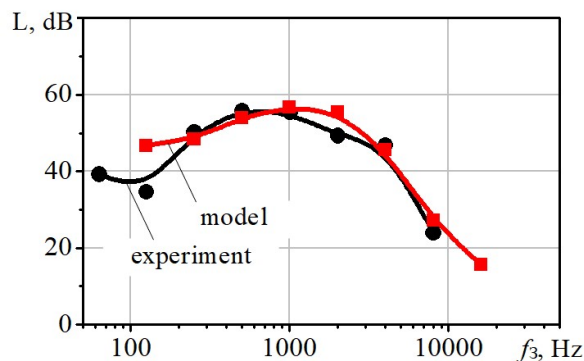


Fig. 12. Influence of sound frequency on sound intensity after passing the panel

## Conclusions

Within the framework of the developed model, the sound absorption efficiency  $\Delta L$  practically does not depend on the initial sound level. Apparently, this is because the model based on linear initial laws (the dependence of the elastic force on displacement and the viscous friction force on velocity) has a linear character.

With a fairly high degree of confidence, it can be argued that in a wide range of sound levels, the PLS panel provides equally effective sound absorption.

## References

1. Utility model patent RU 186420 U1. Lightweight soundproof panel. A.A. Venevitinov, V.F. Asminin, E.V. Druzhinina. - No. 2018136724 dated 17.10.2018; publ. 21.01.2019
2. Rumshisky L.Z. Mathematical processing of experimental results: a reference guide // - Moscow, 1971. - 192 p.
3. Osmolovsky D.S. Reducing noise from round woodworking machines by applying vibration damping friction pads between the saw blade and the clamping flange / D.S. Osmolovsky, V.F. Asminin, E.V. Druzhinina // Akustika. - 2019. - V. 32. - S. 138-140.
4. Asminin V.F. Development and application of a portable lightweight sound suppression panel to reduce noise at permanent and temporary workplaces in the manufacturing and repair workshops / V.F. Asminin, E.V. Druzhinina, D.S. Osmolovsky, S. Sazonova // Akustika. - 2019. - V. 34. - S. 20-23.
5. Tyurina N. Investigation of parameters influencing noise barrier efficiency / N. Tyurina, N. Ivanov, A. Shashurin, S. Bortsova // "Advances in Acoustics, Noise and Vibration - 2021" Proceedings of the 27th International Congress on Sound and Vibration, ICSV 2021. - V. 27. - 2021.
6. Ivanov N. The method of sequential transformation of the sound fields / N. Ivanov, G. Kurtsev, A. Shashurin // Akustika. 2021. - V. 39. - S. 143-149.

7. Butorina M. Noise reduction at workplace in construction / M. Butorina, N. Ivanov, A. Troshchinina // Akustika. 2021. - V. 41. - S. 94-99.

8. Tsukernikov I.E. Determination of noise emission data of construction sites / I.E. Tsukernikov, I.L. Shubin, N.I. Ivanov, T.O. Nevenchannaya, I.A. Nekrasov // Proceedings of Meetings on Acoustics. "Proceedings of Meetings on Acoustics - ICA 2013" 2013. - S. 040085.